Molecular Therapy
Oncolytics
Original Article

AMERICAN SOCIETY of GENE & CELL THERAPY

Sulforaphane Induces miR135b-5p and Its Target Gene, RASAL2, thereby Inhibiting the Progression of Pancreatic Cancer

Libo Yin,[1] Xi Xiao,[1] Christina Georgikou,[1] Yiqiao Luo,[1] Li Liu,[1] Jury Gladkich,[1] Wolfgang Gross,[1] and Ingrid Herr[1]

[1]Molecular OncoSurgery, Section of Surgical Research, Department of General, Visceral, & Transplant Surgery, University of Heidelberg, Heidelberg, Germany

Pancreatic ductal adenocarcinoma (PDA) is one of the most lethal tumors, with poor therapeutic options in the advanced state. The broccoli-derived anti-inflammatory agent sulforaphane was shown to inhibit the progression of pancreatic cancer and other tumor entities. We examined the involvement of pancreatic cancer cell lines were evaluated by microRNA and gene expression arrays, bioinformatics, *in silico* analysis, qRT-PCR, western blotting, immunohistochemistry, *in situ* hybridization, self-renewal and differentiation assays, and *in vivo* xenograft studies. We selected the top nine differentially expressed microRNAs, and miR135b-5p was chosen as the most important candidate for the sulforaphane-induced upregulation of the tumor suppressor gene RASAL2. The expression of miR135b-5p and RASAL2 was almost absent in malignant pancreatic tissues and cell lines, but not in their normal counterparts. Lipofection of miR135b-5p enhanced RASAL2 expression and inhibited ERK1/2 signaling, viability, self-renewal capacity, and tumor growth. These results indicate that miR135b-5p acts as a tumor suppressor via the induction of RASAL2 in PDA.

INTRODUCTION

Pancreatic ductal adenocarcinoma (PDA) is one of the deadliest cancer malignancies and the fourth leading cause of cancer-related death in 2017 in the United States.[1] PDA will be the second cause of cancer mortality in the next decade. Because of an almost late diagnosis in advanced stages, a potential curative surgical intervention is not possible in most cases of PDA. The only therapeutic option remains palliative chemotherapy, despite decades of research.[2] A better understanding of the molecular signaling pathways underlying the progression of PDA may improve this devastating situation.

The anti-inflammatory isothiocyanate sulforaphane, present at a high concentration in broccoli, is considered a promising new therapeutic agent. Recent data have suggested that sulforaphane enhances the therapeutic efficacy of cytotoxic therapy by inhibiting nuclear factor kappa B (NF-κB), which was found to be overactivated in cancer stem-like cells from the pancreas,[3] breast,[4] prostate,[5,6] and other tumor entities.

The RAS protein activator like 2 (RASAL2) protein has been suggested to be a novel tumor suppressor gene for the inhibition of the RAS-extracellular signal-regulated kinase (ERK) pathway, and its expression correlates inversely with stemness and epithelial-mesenchymal transition (EMT) in subcutaneous xenografts or human tissues from bladder and ovarian cancer patients.[7,8] Similarly, RASAL2 expression in human cancer tissues is associated with a better prognosis for patients with renal cell carcinoma,[9] colorectal,[10] or bladder cancer.[9] Conversely, the inhibition of RASAL2 results in the development and progression of cancer of the breast[11] and bladder[7] in mouse models. In patient tissues, RASAL2 mutations have been correlated with advanced stages of breast cancer.[11] Not much has been published about the function of RASAL2 in PDA, but data from the Human Protein Atlas suggest that a high RASAL2 expression correlates with a shorter 5-year survival in 19% of PDA patients, compared with 50% of patients with low RASAL2 expression (https://www.proteinatlas.org/ENSG00000075391-RASAL2/pathology/tissue/pancreatic+cancer#staining).

Several studies have revealed emerging roles for microRNAs (miRNAs) in the regulation of pancreatic cancer progression. These highly conserved, small, 19–25-nucleotide-long, single-stranded, endogenous, noncoding RNAs bind to the 3′ UTR of a target mRNA and have been primarily demonstrated to induce translational suppression or mRNA degradation, resulting in the prevention of protein expression.[12–14] However, a number of studies have revealed that miRNAs can also stimulate gene expression by direct and indirect mechanisms.[8] Depending on the type of miRNA and the cellular context, both anti- and pro-oncogenic effects were observed.[15]

Here, we demonstrate that the expression of miR135b-5p and RASAL2 is low to absent in PDA, in contrast to semi-malignant or normal pancreatic tissue, where the expression is high. By *in situ* hybridization and immunohistochemistry, we identify a positive correlation between miR135b-5p and RASAL2 expression.

Received 16 December 2018; accepted 27 March 2019;
https://doi.org/10.1016/j.omto.2019.03.011.

Correspondence: Ingrid Herr, PhD, Molecular OncoSurgery, Section of Surgical Research, Department of General, Visceral, & Transplant Surgery, University of Heidelberg, Heidelberg, Germany.
E-mail: i.herr@uni-heidelberg.de

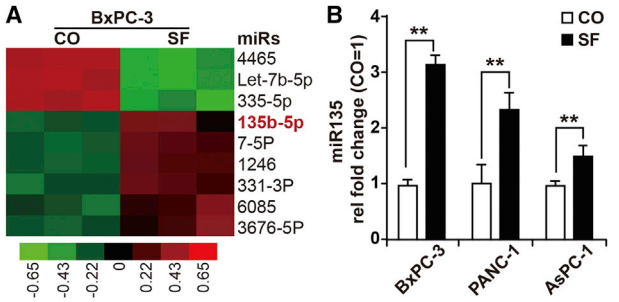

Figure 1. Sulforaphane Upregulates miR-135b-5p

(A) BxPC-3 cells were treated with 10 μM sulforaphane (SF) or were left untreated (control [CO]). Total RNA was harvested 24 h later and used for GeneChip miRNA 4.0 Array in triplicate. The heatmap presents the nine most significantly up- and downregulated miRNAs. The red color marks high expression, and the green color marks low expression within a scale from 0.65 to −0.65, as indicated. (B) BxPC-3, PANC-1, and AsPC-1 cells were treated as described above, and 24 later, the RNA was harvested, and the fold change in miR135b-5p expression was determined by qRT-PCR and normalized to RNU6B. The mean fold change in the control was set to 1. Means ± SD are shown; **p < 0.01.

RESULTS

Sulforaphane Enhances the Expression of miR-135b-5p

To detect the sulforaphane-induced differential regulation of miRNAs, total RNA from BxPC-3 cells was collected at 24 h after treatment with 10 μM sulforaphane, and miRNA microarray expression profiling was performed. Based on bioinformatics evaluation, the nine most significantly differentially regulated miRNAs were selected and are shown in a heatmap (Figure 1A). Whereas miR-135b-5p, miR-7-5p, miR-1246, miR-331-3p, miR-6085, and miR-3676-5p were upregulated, miR-4465, Let-7b-5p, and miR-335-5p were downregulated. To identify new miRNAs related to pancreatic cancer progression, a literature search was performed in PubMed and Web of Science with the keywords "pancreatic cancer," "miRNAs," and "patient." A few miRNAs, whose differential expression between normal and malignant pancreatic tissue has already been experimentally confirmed, were identified (Table S1). By comparing these results with the top candidates of the miRNA array, we selected miR135b-5p as the most relevant. To confirm the sulforaphane-induced differential regulation of miR135b-5p expression, RNA from untreated and sulforaphane-treated BxPC-3, PANC-1, and AsPC-1 cells was harvested and analyzed by qPCR. The results confirmed that the expression of miR135b-5p was significantly increased upon sulforaphane treatment (Figure 1B).

Overexpression of miR135b-5p Inhibits Self-Renewal Capacity

To evaluate whether miR135b-5p mimicked the known inhibitory effects of sulforaphane on PDA progression features, miR135b-5p mimics or mock control mimics were transfected by liposomes into BxPC-3, PANC-1, and AsPC-1 cells. Twenty-four hours later, the expression of miR135b-5p was determined by qPCR analysis (Figure S1), which confirmed its high overexpression by factors of 10,000, 250, and 20,000, respectively. The overexpression of miR135b-5p was reflected by a strong repression of viability (Figure 2A), migratory activity (Figure 2B), and colony-forming capacity (Figure 2C).

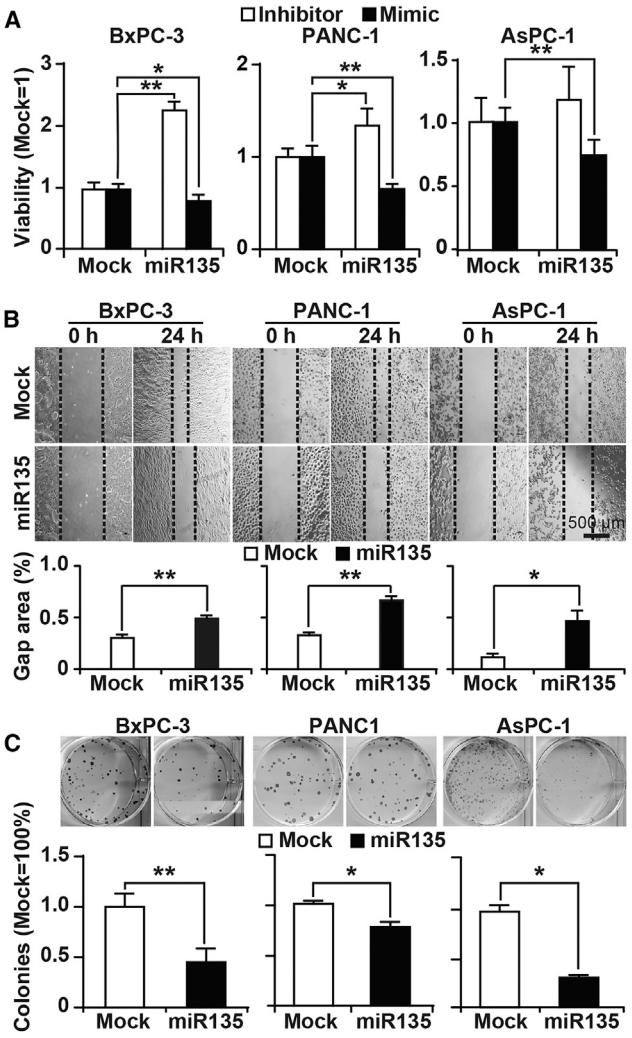

Figure 2. miR135b-5p Inhibits Progression Features

BxPC-3, PANC-1, and AsPC-1 cells were lipofected with 50 nM miR135b-5p mimic (miR135) or a nonsense miRNA control (mock). (A) Using these cells, the viability was detected by MTT assay 24 h after transfection. (B) Similarly, 24 h after lipofection, the cells were seeded onto 6-well plates and cultured until they reached 90% confluence. Then, a line was scratched into the middle of the cell layer with a 10-μL pipette tip. The closure of the wounded region was evaluated and recorded by microscopy at ×100 magnification. The size of the gap area was calculated by ImageJ software and by detecting the square of length × width. (C) Similarly, 24 h after transfection, the cells were reseeded at a low density (BxPC-3: 1,000 cells/well; PANC-1: 500 cells/well; and AsPC1: 300 cells) and cultured for 2 weeks in regular culture medium. Then, the cells were fixed and stained with Coomassie, followed by the evaluation of colonies comprising at least 50 cells. The number of colonies in the mock group was set to 1. Colonies containing more than 50 cells were treated as a single colony. The clonogenicity efficiency was calculated (number of colonies/number of seeded cells) × 100. Means ± SD are shown; *p < 0.05, **p < 0.01.

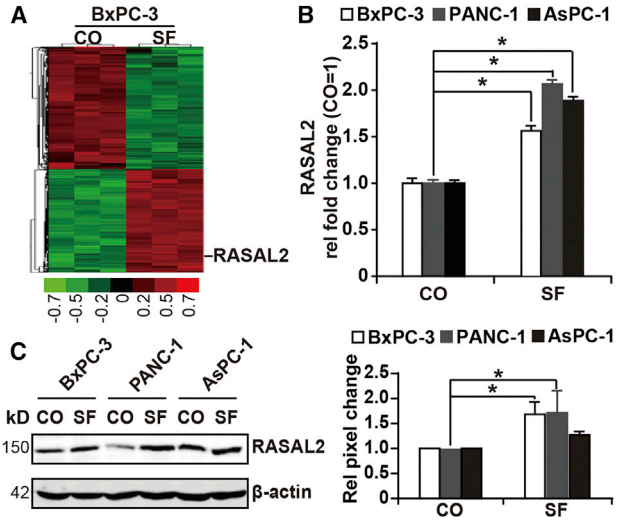

Figure 3. miR135b-5p Regulates RASAL2

(A) BxPC3 cells were treated with 10 μM sulforaphane (SF) or were left untreated (CO). Twenty-four hours later, mRNA was harvested, followed by gene expression profiling in triplicate using the GeneChip miRNA 4.0 Array. A heatmap of candidate mRNAs was created, which combined the array and database results. The most significant upregulated candidate gene RASAL2 is marked. The scale from −0.7 to 0.7 marks the intensity of differential regulation of genes: high expression (red), middle expression (black), and low expression (green). (B) BxPC-3, PANC-1, and AsPC-1 cells were treated as described above, and RNA was harvested. The fold change in RASAL2 expression was determined by qRT-PCR and normalized to GAPDH. The controls were set to 1. (C) The cells were treated as described above, followed by harvest of the proteins 24 h later and examination of RASAL2 protein expression by western blot analysis. The expression of β-actin served as a control for equal conditions. The band intensities (pixel intensities) were measured using ImageJ and are shown in the diagram on the left, after normalization to β-actin. Means ± SD are shown; *$p < 0.05$, **$p < 0.01$.

miR135b-5p Promotes RASAL2 Expression

To detect the putative target genes of sulforaphane, which could be regulated by miR-135b-5p, we collected total RNA from BxPC-3 cells at 24 h after treatment with sulforaphane and performed mRNA microarray expression profiling. Compared to untreated control cells, we found the differential expression of 711 mRNAs ($p < 0.01$). Among these mRNAs, 396 were downregulated and 315 were upregulated, as shown in the heatmap (Figure 3A) and Table S2. Among these genes, RASAL2 was considered the most interesting for functional reasons. The upregulation of RASAL2 mRNA and protein by sulforaphane was confirmed in BxPC-3, PANC-1, and AsPC-1 cells by qRT-PCR (Figure 3B) and western blot analysis (Figure 3C).

To identify whether RASAL2 was targeted by miR-135b-5p, we analyzed the mRNA microarray results *in silico* with the miRWalk database, which predicted 51 miR135b-5p target genes, among which was RASAL2 (Table S3). By using the TargetScan online database,[16] we identified 2 putative miR135b-5p-binding sites in the RASAL2 3′ UTR (Figure 4A), which is a regulatory element in the mRNA sequence that immediately follows the translation termination code.[17] To examine whether miR135b-5p indeed regulates RASAL2, BxPC-3 and PANC-1 cells were lipofected with miR135b-5p or mock control mimics. Twenty-four hours later, total RNA was harvested, and the mRNA expression of RASAL2 was measured by qRT-PCR. The overexpression of miR135b-5p led to an increase in RASAL2 of 55% and 70% in the cell lines, respectively, compared to that in the mock control (Figure 4B). Similar results were found by immunohistochemistry (Figure 4C).

miR135b-5p Inhibits the Growth of Tumor Xenografts *In Vivo*

To evaluate the *in vivo* relevance of these findings, we transfected BxPC-3 cells with miR135b-5p mimics or mock control mimics and transplanted these cells onto the chorioallantoic membranes of fertilized chicken eggs on day 9 of development and resected the tumor xenografts on day 18. The size of each xenograft tumor was measured by calipers, and representative tumors, the size of each tumor and the mean sizes are shown (Figure 5A). There was a significantly smaller size of the xenograft tumors from miR-135b-5p-overexpressing cells. This effect is most likely due to the overexpression of RASAL2 in the respective xenografts, as confirmed by qRT-PCR analysis and immunofluorescence staining from xenograft tissue (Figures 5B and 5C). To further highlight the effect of miR135b-5p on proliferation, we stained tumor sections for the proliferation marker Ki67 and found a significant reduction in proliferation (Figure 5D). Similarly, the cleaved fragment of activated caspase-3 was significantly upregulated in miR-135b-5p-overexpressing cells, indicating enhanced apoptosis (Figure 5E). In addition, miR135b-5p reduced the phosphorylation of the RASAL2 target pERK and the expression of the stemness and EMT markers Vimentin, CD133, and CD44, whereas E-cadherin expression was upregulated (Figure 5F). These results indicate that miR135b-5p inhibited tumor progression most likely via RASAL2.

Correlation of miR135b-5p and RASAL2 Expression in Patient Tissue

Finally, to verify the relevance of these findings for patients, we detected the expression of miR135b-5p and RASAL2 in the tissues of highly aggressive PDA (n = 6), less malignant intraductal papillary mucinous neoplasm (IPMN; n = 6), and nonmalignant pancreas (n = 6) tissue samples by *in situ* hybridization and immunohistochemistry (Figure 6A; Table S4). The expression patterns and the number of positive cells were evaluated blindly by two experienced scientists. Whereas the expression of miR135b-5p and RASAL2 was highest in normal pancreatic tissues, the expression was lower in IPMN tissue and very low to absent in PDA tissue. These results were quantified by grading the expression intensity of miR-135b-5p, which decreased significantly with increasing malignancy. Non-parametric tests (Kruskal-Wallis and Mann-Whitney) were performed over all groups with p values < 0.05, suggesting a strong negative correlation between miR-135b-5p expression and malignancy (Figure 6B). A similar strong negative correlation was found for RASAL2 expression with a p value of < 0.01, suggesting that RASAL2 expression correlates negatively with malignancy (Figure 6C). The documentation of RASAL2 and miR135b-5p in a

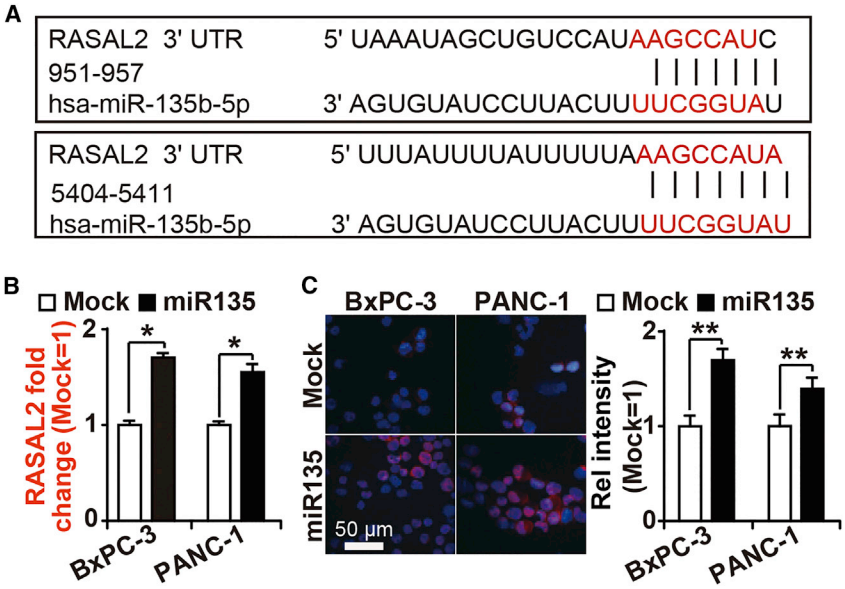

Figure 4. Sulforaphane Increases RASAL2 Expression
(A) Scheme of the miR135b-5p 5′ seed region and two complementary sequences in the RASAL2 3′ UTR. (B) Total mRNA was harvested from BxPC-3 and PANC-1 cells, which were transfected with miR135b-5p or a noncoding miRNA control (mock), and the mRNA expression of RASAL2 was validated by qRT-PCR, as described in Figure 3B. (C) The expression of RASAL2 was examined in BxPC-3 and PANC-1 cells 24 h after transfection, as described above, by staining with a specific antibody (violet), counterstaining with DAPI (blue), and detection with fluorescence microscopy. Representative images of each group are shown at ×100 magnification, and the bar indicates 50 μm. The relative fluorescence intensity was examined at ×400 magnification with a Leica DMRB fluorescence microscope and quantified with ImageJ. The control was set to 1. Means ± SD are shown on the right and in the diagram; *$p < 0.05$, **$p < 0.01$.

scatterplot (Figure 6D) confirmed the relation of the expression of these factors with the grade of malignancy—namely, an absence of expression in highly malignant PDA, low to high expression in low to highly malignant IPMN, and high expression in non-malignant normal pancreatic tissue. Together, these data suggest, that low to absent expression of RASAL2 and miR-135b-5p are indicators of the grade of malignancy in pancreatic cancer.

DISCUSSION

In this study, we observed that the bioactive agent sulforaphane induces the upregulation of miR-135b-5p, which in turn upregulates the novel tumor suppressor RASAL2. We found that both factors are inhibited in highly aggressive pancreatic cancer cell lines and tissues and that their absence correlates with malignancy. We observed median expression levels in less aggressive IPMN tissues and strong expression levels in nonmalignant pancreatic tissues. By the mimic-mediated overexpression of miR135b-5p, we found that progression features *in vitro* and tumor growth *in vivo* were strongly inhibited. Conversely, the siRNA-mediated inhibition of RASAL2 activated ERK activity, and the overexpression of miR135b-5p inhibited it. Therefore, we suggest the miR135b-5p/RASAL2 signaling cascade as a new tumor suppressor system for the inhibition of the ERK-mediated progression of pancreatic cancer.

Our results demonstrated the upregulation of RASAL2 by miR135b-5p. This mechanism is different from the usual mechanism of action of miRNAs, which have primarily been demonstrated to mediate the transcriptional or post-transcriptional downregulation of target genes through binding of the 3′ UTR of the mRNA to the miRNA seed region.[18–20] However, a number of studies have shown that miRNAs can also mediate transcriptional gene activation instead of gene silencing.[8] The first miRNA identified as an activator of a target gene was human miR-373, which induced the transcription of E-cadherin and CSDC2.[21] Additionally, several reports, including ours, have confirmed the observation of miRNA-induced transcriptional activation, suggesting the existence of a new and widespread mechanism of action for miRNAs whose underlying biochemical processes are still unknown.[22] However, the presence of a DNA sequence complementary to the 5′ seed region and partially to the flanking region of miRNA is required for transcriptional activation. Because we identified a seed region in the miR135b-5p 5′ end that is complementary to two sequences within the 3′ UTR region of RASAL2, we assume that binding plays a role in the transcriptional upregulation of RASAL2 in our system. According to a suggested mechanism,[8] miR135b-5p may function in concert with particular messenger ribonucleoprotein complexes and in response to specific cellular conditions to activate the expression of RASAL2.

Our results reveal that RASAL2 acts as a tumor suppressor in pancreatic cancer because its expression correlated with low or absent malignancy, whereas low or absent RASAL2 expression correlated with highly aggressive pancreatic cancer. This study is the first to show the function of RASAL2 as a tumor suppressor in PDA. Our data are in line with the findings in other tumor entities, because a tumor suppressor function for RASAL2 has been described in cancers of the bladder, ovaries, kidney, breast, and colorectal.[7,8,10,11] In our study, we verified that RASAL2 inhibits ERK phosphorylation and features of tumor progression and the EMT by siRNA-mediated inhibition of RASAL2 by the miR135b-5p-mediated expression of RASAL2. On the other hand, RASAL2 expression has been described to act in an oncogenic manner in triple-negative breast cancer and in ovarian cancer to drive mesenchymal invasion and metastasis.[23,24] We do not know the reason for these opposing results, but we assume that they may have reflected differences in the tumor microenvironments.

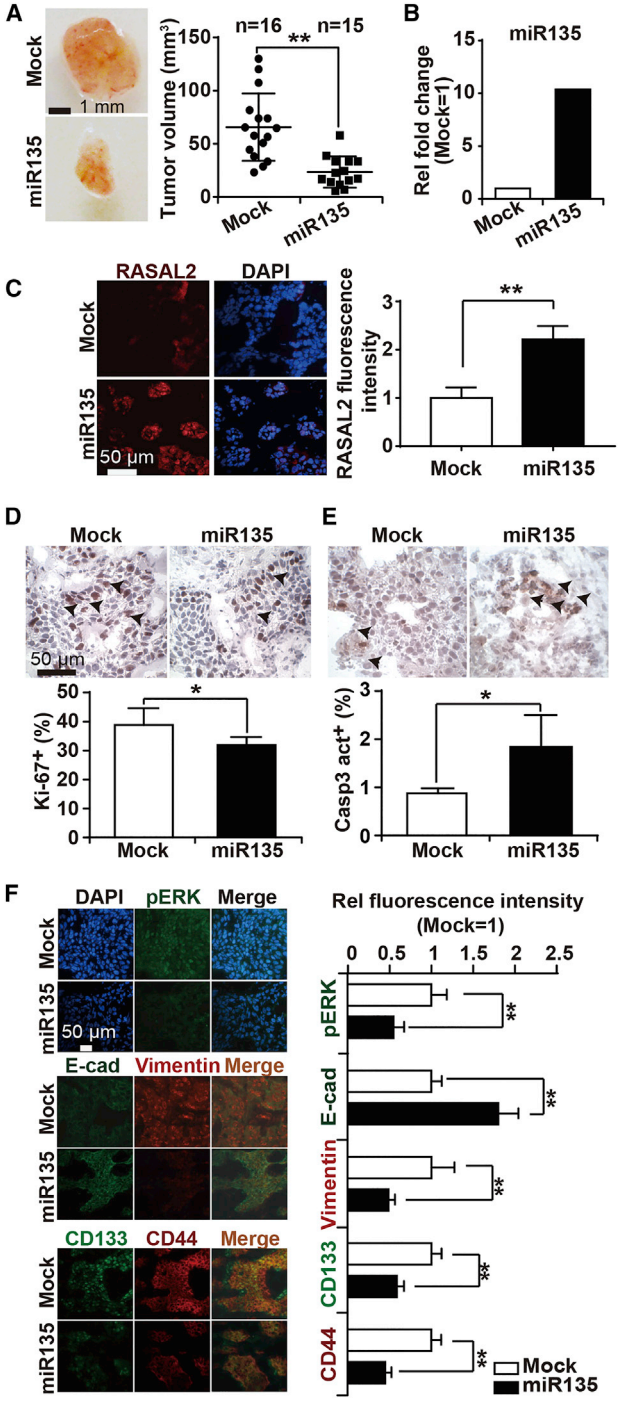

Figure 5. miR135b-5p Reduces the Volume of Xenograft Tumors

BxPC-3 cells were transfected with miR135b-5p (miR135) mimics or a nonsense miRNA control (mock) as described in detail in Figure 2. Twenty-four hours after transfection, the cells were transplanted onto the chorioallantoic membrane of fertilized chicken eggs on day 9 of embryonic development. Nine days later, on day 18 of development, the chick embryos were euthanized, followed by the resection of the xenografts and measurement of the size by calipers. (A) Representative tumor xenografts are shown on the left, and the individual tumor sizes and their means are presented on the right; $^{**}p < 0.01$. (B) RNA was harvested from xenograft tissue, and RASAL2 mRNA expression was measured by qRT-PCR, as described in Figure 3B. (C) RASAL2 protein expression was detected in cryosections from xenograft tissue by immunofluorescence microscopy. Representative stained images are shown on the left. The relative fluorescence intensity was examined at ×400 magnification, using a Leica DMRB fluorescence microscope and ImageJ. The control was set to 1. means ± SD are shown on the right; $^{**}p < 0.01$. Similarly, the expression of the proliferation marker Ki-67 (D) and of the apoptosis marker "cleaved fragment of caspase-3" (Casp3 act$^+$) (E) was detected by immunohistochemistry. Representative staining images are shown on the top. Positive cells appear red to dark red and are marked by black arrows. The percentage of positive cells was defined by counting the number of positive cells in 10 randomly chosen areas, and the means ± SD are shown on the bottom; $^{*}p < 0.05$. (F) Immunofluorescence staining of phosphorylated ERK 1/2 (pERK), Vimentin, E-cadherin (E-cad), CD133, and CD44 and counterstaining of the nuclei with DAPI (blue). Overlays (Merge) of phosphorylated ERK 1/2 with DAPI, of E-cadherin with Vimentin and of CD133 with CD44 are shown on the left. The relative fluorescence intensity was examined as described above.

This inconsistency of RASAL2 function is reflected by the controversial functions of miR135 in various cancers. According to our data, miR135 has a tumor suppressor function in pancreatic cancer. This result is in line with data found in breast cancer, where miR135 impaired progression by the downregulation of FAK or Runx2,[25,26] and the data obtained in prostate cancer, where miR135a-1 inhibited progression by the downregulation of epidermal growth factor receptor (EGFR).[27] On the other hand, miR135 is suggested as an oncogene in (1) melanoma cells by the downregulation of Forkhead Box O1 (FOXO1),[28] (2) non-small-cell lung cancer by the downregulation of tripartite motif containing 16 (TRIM16),[29] and (3) esophageal squamous cell carcinoma by the downregulation of RERG.[30] Thus, miR135 has several different cellular target genes and its function as a tumor suppressor or oncogene seems to depend on the tumor entity and cellular context.

Finally, we would like to mention that, although mice are the most common animal models used for miRNA delivery, we used a chicken egg xenotransplantation model. This was not only due to the high costs and administrative and ethical barriers of mouse studies, but was also because the chicken egg model is an excellent alternative, which has been evaluated in several of our recent studies,[11,31,32] which can be easily used for the delivery of miRNA *in vivo*.[18] Chicken eggs are naturally immunodeficient and the blood vessel network of the chorioallantoic membrane (CAM) supports the growth of a tumor xenograft. A major advantage is that the CAM is noninnervated and allows painless tumor inoculation and growth and CAM injections. In addition, tumors grow much faster on chicken eggs than on mice, the tumor xenografts have a well-developed histopathological morphology with tumor microenvironment, and the CAM model can be easily performed in any laboratory, as the method is inexpensive, and an animal application is not required until day 18 of embryonic chick development. Therefore, we feel that the chicken egg xenotransplantation model is well suited for short-term *in vivo* xenograft growth for up to 10 days.

In conclusion, low to absent miR135b-5p and RASAL2 expression levels correlate with the median to high malignancy of pancreatic

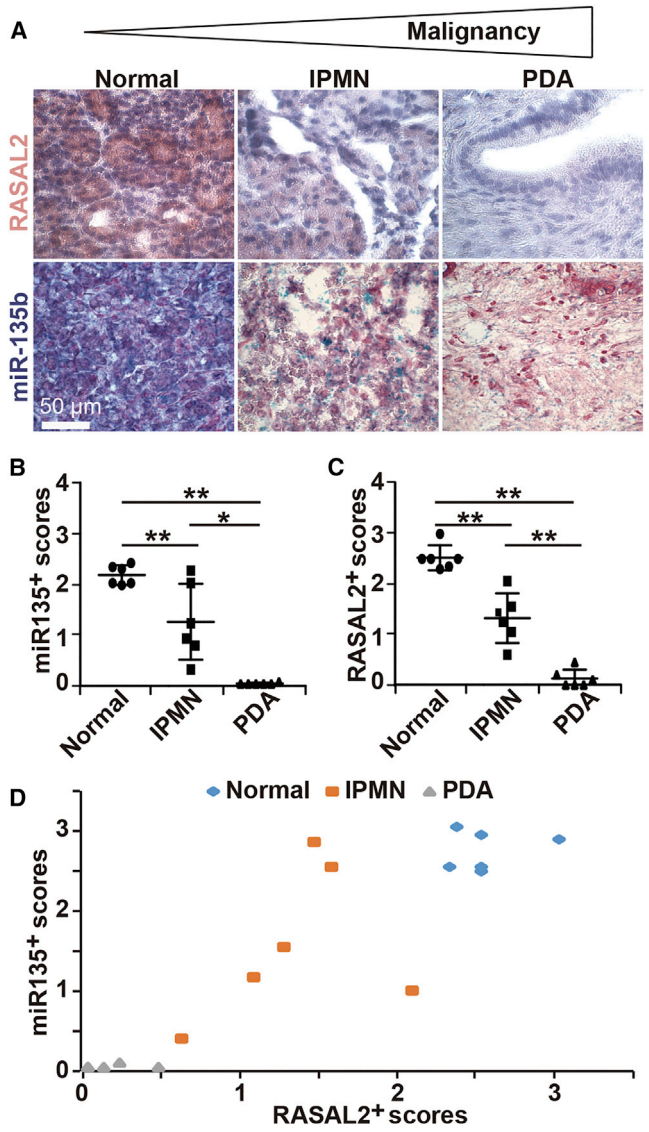

Figure 6. Correlation of miR-135b-5p and RASAL2 Expression

(A) Paraffin-embedded specimens from PDA (n = 6), IPMN (n = 6), or normal tissue (n = 6) were examined by immunohistochemistry for expression of RASAL2 and by *in situ* hybridization for the expression of miR135b-5p (miR135). Representative pictures are shown at ×100 magnification. The bar indicates 50 μm. Positively stained images of RASAL2 appear brown and images of miR135b-5p appear black-purple. (B) The expression levels of RASAL2 and (C) of miR135b-5p were quantified by counting the positively stained cells in 10 randomly chosen microscopic visual fields of each tissue. High expression levels were scored as 3, medium expression levels as 2, low expression levels as 1, and the absence of expression as 0. The means of the scores per tissue are shown in the scatterplots. (D) The expression scores of miR135b-5p and RASAL2 are shown as a scatterplot, and the plots of normal, IPMN, and PDA tissue are marked in color.

cancer, whereas the median or high expression of these two factors correlates with less malignant or nonmalignant pancreatic tissue. These effects are due to miR135b-5p-induced RASAL2 expression, which inhibits ERK signaling and cancer progression. The broccoli bioactive agent sulforaphane restored miR135b-5p and RASAL2 expression in PDA, suggesting that a diet rich in broccoli and other vegetables of the cruciferous family may support conventional PDA therapy.

MATERIALS AND METHODS

Tumor Cell Lines

The established human PDA cell lines AsPC-1, BxPC-3, PANC-1, and MIA-PaCa2 were purchased from the American Type Culture Collection (ATCC, Manassas, VA, USA). The cells were cultured in DMEM with high glucose (Sigma-Aldrich, Muenchen, Germany), supplemented with 10% fetal calf serum (FCS; Sigma-Aldrich) and 1 mM HEPES (PAA Laboratories, Posching, Austria). All cell lines were authenticated by a commercial institution (Multiplexion, Heidelberg, Germany), and mycoplasma was tested monthly by PlasmoTest (InvivoGen, San Diego, CA, USA). BxPC-3 and Bx-Gem cells were cultured in DMEM supplemented with 10% FCS and 25 mmol/L HEPES (Thermo Fisher, Dreieich, Germany).

Patient Tissue

Patient tissues were obtained under the approval of the Ethics Committee of the University of Heidelberg after receiving written informed consent from the patients. The diagnoses were established by conventional clinical and histological criteria according to the World Health Organization (WHO). All surgical resections were indicated by the principles and practice of oncological therapy.

Reagents

Sulforaphane (≥95%) and the ERK inhibitor FR180204 (Sigma-Aldrich, St. Louis, MO, USA) were prepared in DMSO to 100 and 50 mM stock solutions, respectively, and stored in aliquots at −20°C. Each aliquot was used only once, immediately after thawing. The final concentrations of the solvents in media were 0.1% or less.

Xenotransplantation into Chicken Eggs

Briefly, treated cells were seeded onto a CAM on day 9 of development of the chicken embryo, followed by treatment and analysis of the tumor volume and side effects as previously described.[33]

Cell Viability

PDA cells were resuspended at a final concentration of 4×10^4–10^5/mL and plated onto 96-well microplates at 100 μL per well. After treatment, the cell viability was examined by tetrazolium dye MTT 3-(4,5-dimethylthiazol-2-yl)-2,5-diphenyltetrazolium bromide (MTT) assay, as previously described.[31]

Colony-Forming Assay

Twenty-four hours after treatment, the cells were seeded at low density onto 6-well plates. The colony-forming capacity was evaluated at 14 days later, as previously described.[3]

Wound-Healing Assay

After transfection, the cells were seeded onto 6-well plates and incubated at 37°C until 90% confluence was reached. A cross was

scratched into the cell layer with 10-μL pipette tip. Twenty-four hours after incubation, photos of the wounded areas were taken, and the gap area was quantified by ImageJ software.

Western Blot Analyses

Western blot analyses were performed as previously described.[3] The following antibodies (Abs) were used: rabbit polyclonal Abs against RASAL2 (82481, 1:1,000; Cell Signaling Technology, Danvers, MA, USA) and mouse monoclonal Abs against β-actin (A1978, 1:5,000; Sigma-Aldrich, St. Louis, MO, USA).

Immunohistochemical and Immunofluorescence Staining

Staining was performed on frozen tissue sections or established cell lines, as previously described.[3] The following Abs were used: mouse monoclonal Abs against RASAL2 (sc-390605, 1:100; Santa Cruz, Dallas, TX, USA), Vimentin (ab8069, 1:200; Abcam, Cambridge, UK), and Erk1/2 (9106, 1:200; Cell Signaling Technology, Danvers, MA, USA); rabbit monoclonal Ab against E-cadherin (3195, 1:200; Cell Signaling Technology); and rabbit polyclonal Abs against CD133 (ab16518, 1:400; Abcam), CD-44 (ab51037, 1:100; Abcam), and phospho-Erk1/2 (4370, 1:200; Cell Signaling Technology).

mRNA and miRNA Profiling

GeneChip Human Gene 2.0 ST Array (Thermo Fisher Scientific, Carlsbad, CA, USA) and GeneChip miRNA 4.0 Array (Thermo Fisher) were used for mRNA and miRNA profiling, respectively. The analysis and bioinformatic evaluation were performed at the Mannheim Medical Research Center, University of Heidelberg. The array data were uploaded to array express. The accession numbers are ArrayExpress: E-MTAB-7559 (for mRNA profiling) and E-MTAB-7560 (for miRNA profiling).

MicroRNA and siRNA Transfection

MirVana mimics and nonsense miRNA control (mock) mimics (Thermo Fisher, Dreieich, Germany) were transfected with Lipofectamine 2000 (Thermo Fisher, Dreieich, Germany) at a concentration of 50 nM, according to the manufacturer's instructions. Similarly, RASAL2 siRNA (Thermo Scientific, Rochester, NY, USA) at a concentration of 50 nM was lipofected, and the Silencer Negative Control siRNA (Thermo Scientific, Rochester, NY, USA) served as a control.

miRNA and mRNA Extraction and qRT-PCR

The RNeasy Mini Kit and the miRNeasy Mini Kit (QIAGEN, Hilden, Germany) were used for the isolation of mRNA and miRNA, respectively. TaqMan Small RNA Assays and TaqMan Gene Expression Assays (Thermo Fisher, Darmstadt, Germany) were used for qRT-PCR according to the manufacturer's instructions. miR-135b-5p, RASAL2, and the control primers RNU6B and GAPDH were purchased ready to use from Thermo Fisher.

Detection of miR135b-5p Expression by *In Situ* Hybridization

The detection of miR135b-5p expression in tissue sections was performed using the miRCURY LNA microRNA Detection Kit (QIAGEN, Hilden, Germany) as described.[32] Staining was performed on formalin-fixed, paraffin-embedded patient tissues. Briefly, the sections were dewaxed in Roti-Histol (Carl Roth, Karlsruhe, Germany, rehydrated in 2-propanol, treated with proteinase K (15 mg/mL; QIAGEN, Hilden, Germany) and air dried. Hybridization was performed for 2 h at 52°C, using a miR-135b-5p-specific sequence; the sequence of the digoxigenin-labeled locked nucleic acid (LNA) detection probe was 5′- TCACATAGGAATGAAAAGCCA-3′. A scrambled miRNA probe was used as a negative control. After stringent washes, the bound LNA probes were detected with alkaline phosphatase-conjugated digoxigenin Ab (Roche Diagnostics, Mannheim, Germany) and nitroblue tetrazolium/5-bromo-4-chloro-3'-indolyphosphate p-toluidine (NBT/BCIP; Vector Laboratories, Burlingame, CA, USA) as the substrate. Nuclear Fast Red (Vector Laboratories, Burlingame, CA, USA) was used for nuclear staining. The sections were mounted using Roti-Mount FluorCare.

Statistical Analysis

Data obtained with established cell lines are presented as means ± SD from three separate experiments performed at least in triplicate. The significance of the data was analyzed using Student's t test for parametric data and the Mann-Whitney test for nonparametric data. The Pearson product-moment correlation was performed to measure the linear correlation between two variables x and y. Regarding the immunohistochemistry or immunofluorescence experiments, the expression intensity and the percentage of positive cells were determined by counting the number of differentiated cells in 10 fields of view for each group. $p < 0.05$ was considered statistically significant ($^*p < 0.05$, $^{**}p < 0.01$).

Declarations

Ethical Approval and Consent to Participate

Patient materials were obtained under the approval of the Ethics Committee of the University of Heidelberg after receiving written informed consent from the patients. The diagnoses were established by conventional clinical and histological criteria according to the World Health Organization (WHO). All surgical resections were indicated by the principles and practice of oncological therapy.

Consent for Publication

All authors agree with the publication of this manuscript. This manuscript has not been published and is not under consideration for publication elsewhere.

Availability of Supporting Data

The datasets supporting the conclusions of this article are included within the article, and its supplemental files and are thus available.

SUPPLEMENTAL INFORMATION

Supplemental Information can be found online at https://doi.org/10.1016/j.omto.2019.03.011.

AUTHOR CONTRIBUTIONS

Concept and Design, I.H. and L.Y.; Development of Methodology, L.Y., X.X., and C.G.; Acquisition of Data, L.Y., X.X., C.G., and J.G.;

Analysis and Interpretation of Data, L.Y., Y.L., W.G., and I.H.; Writing – Reviewing and/or Revising, L.Y. and I.H.

CONFLICTS OF INTEREST

None of the authors has a conflict of interest to disclose regarding the publication of the present manuscript.

ACKNOWLEDGMENTS

We are grateful to S. Bauer for excellent technical assistance. This study was supported by the China Scholarship Council, by a scholarship to L.Y., and by grants to I.H. from the German Cancer Aid (Deutsche Krebshilfe 111299), German Research Council (DFG HE 3186/15-1), the Heidelberger Stiftung Chirurgie, the Dietmar Hopp-Stiftung, the Klaus Tschira Stiftung, and the Hanns A. Pielenz-Stiftung.

REFERENCES

1. Siegel, R.L., Miller, K.D., and Jemal, A. (2017). Cancer Statistics, 2017. CA Cancer J. Clin. *67*, 7–30.
2. Strobel, O., Neoptolemos, J., Jager, D., and Buchler, M.W. (2019). Optimizing the outcomes of pancreatic cancer surgery. Nat. Rev. Clin. Oncol. *16*, 11–26.
3. Kallifatidis, G., Rausch, V., Baumann, B., Apel, A., Beckermann, B.M., Groth, A., Mattern, J., Li, Z., Kolb, A., Moldenhauer, G., et al. (2009). Sulforaphane targets pancreatic tumour-initiating cells by NF-kappaB-induced antiapoptotic signalling. Gut *58*, 949–963.
4. Li, Y., Zhang, T., Korkaya, H., Liu, S., Lee, H.F., Newman, B., Yu, Y., Clouthier, S.G., Schwartz, S.J., Wicha, M.S., and Sun, D. (2010). Sulforaphane, a dietary component of broccoli/broccoli sprouts, inhibits breast cancer stem cells. Clin. Cancer Res. *16*, 2580–2590.
5. Kallifatidis, G., Labsch, S., Rausch, V., Mattern, J., Gladkich, J., Moldenhauer, G., Büchler, M.W., Salnikov, A.V., and Herr, I. (2011). Sulforaphane increases drug-mediated cytotoxicity toward cancer stem-like cells of pancreas and prostate. Mol. Ther. *19*, 188–195.
6. Labsch, S., Liu, L., Bauer, N., Zhang, Y., Aleksandrowicz, E., Gladkich, J., Schönsiegel, F., and Herr, I. (2014). Sulforaphane and TRAIL induce a synergistic elimination of advanced prostate cancer stem-like cells. Int. J. Oncol. *44*, 1470–1480.
7. Hui, K., Gao, Y., Huang, J., Xu, S., Wang, B., Zeng, J., Fan, J., Wang, X., Yue, Y., Wu, S., et al. (2017). RASAL2, a RAS GTPase-activating protein, inhibits stemness and epithelial-mesenchymal transition via MAPK/SOX2 pathway in bladder cancer. Cell Death Dis. *8*, e2600.
8. Vasudevan, S. (2012). Posttranscriptional upregulation by microRNAs. Wiley Interdiscip. Rev. RNA *3*, 311–330.
9. Hui, K., Wu, S., Yue, Y., Gu, Y., Guan, B., Wang, X., Hsieh, J.T., Chang, L.S., He, D., and Wu, K. (2018). RASAL2 inhibits tumor angiogenesis via p-AKT/ETS1 signaling in bladder cancer. Cell. Signal. *48*, 38–44.
10. Pan, Y., Tong, J.H.M., Lung, R.W.M., Kang, W., Kwan, J.S.H., Chak, W.P., Tin, K.Y., Chung, L.Y., Wu, F., Ng, S.S.M., et al. (2018). RASAL2 promotes tumor progression through LATS2/YAP1 axis of hippo signaling pathway in colorectal cancer. Mol. Cancer *17*, 102.
11. McLaughlin, S.K., Olsen, S.N., Dake, B., De Raedt, T., Lim, E., Bronson, R.T., Beroukhim, R., Polyak, K., Brown, M., Kuperwasser, C., and Cichowski, K. (2013). The RasGAP gene, RASAL2, is a tumor and metastasis suppressor. Cancer Cell *24*, 365–378.
12. Ha, M., and Kim, V.N. (2014). Regulation of microRNA biogenesis. Nat. Rev. Mol. Cell Biol. *15*, 509–524.
13. Calin, G.A., and Croce, C.M. (2006). MicroRNA signatures in human cancers. Nat. Rev. Cancer *6*, 857–866.
14. Zhu, M., Xu, Z., Wang, K., Wang, N., and Li, Y. (2013). microRNA and gene networks in human pancreatic cancer. Oncol. Lett. *6*, 1133–1139.
15. Iorio, M.V., and Croce, C.M. (2012). MicroRNA dysregulation in cancer: diagnostics, monitoring and therapeutics. A comprehensive review. EMBO Mol. Med. *4*, 143–159.
16. Agarwal, V., Bell, G.W., Nam, J.W., and Bartel, D.P. (2015). Predicting effective microRNA target sites in mammalian mRNAs. eLife *4*, 05005.
17. Barrett, L.W., Fletcher, S., and Wilton, S.D. (2012). Regulation of eukaryotic gene expression by the untranslated gene regions and other non-coding elements. Cell. Mol. Life Sci. *69*, 3613–3634.
18. Gulyaeva, L.F., and Kushlinskiy, N.E. (2016). Regulatory mechanisms of microRNA expression. J. Transl. Med. *14*, 143.
19. Gebert, L.F.R., and MacRae, I.J. (2019). Regulation of microRNA function in animals. Nat. Rev. Mol. Cell Biol. *20*, 21–37.
20. Fabian, M.R., and Sonenberg, N. (2012). The mechanics of miRNA-mediated gene silencing: a look under the hood of miRISC. Nat. Struct. Mol. Biol. *19*, 586–593.
21. Place, R.F., Li, L.C., Pookot, D., Noonan, E.J., and Dahiya, R. (2008). MicroRNA-373 induces expression of genes with complementary promoter sequences. Proc. Natl. Acad. Sci. USA *105*, 1608–1613.
22. Catalanotto, C., Cogoni, C., and Zardo, G. (2016). MicroRNA in Control of Gene Expression: An Overview of Nuclear Functions. Int. J. Mol. Sci. *17*, E1712.
23. Feng, M., Bao, Y., Li, Z., Li, J., Gong, M., Lam, S., Wang, J., Marzese, D.M., Donovan, N., Tan, E.Y., et al. (2014). RASAL2 activates RAC1 to promote triple-negative breast cancer progression. J. Clin. Invest. *124*, 5291–5304.
24. Huang, Y., Zhao, M., Xu, H., Wang, K., Fu, Z., Jiang, Y., and Yao, Z. (2014). RASAL2 down-regulation in ovarian cancer promotes epithelial-mesenchymal transition and metastasis. Oncotarget *5*, 6734–6745.
25. Golubovskaya, V.M., Sumbler, B., Ho, B., Yemma, M., and Cance, W.G. (2014). MiR-138 and MiR-135 directly target focal adhesion kinase, inhibit cell invasion, and increase sensitivity to chemotherapy in cancer cells. Anticancer. Agents Med. Chem. *14*, 18–28.
26. Taipaleenmäki, H., Browne, G., Akech, J., Zustin, J., van Wijnen, A.J., Stein, J.L., Hesse, E., Stein, G.S., and Lian, J.B. (2015). Targeting of Runx2 by miR-135 and miR-203 Impairs Progression of Breast Cancer and Metastatic Bone Disease. Cancer Res. *75*, 1433–1444.
27. Xu, B., Tao, T., Wang, Y., Fang, F., Huang, Y., Chen, S., Zhu, W., and Chen, M. (2016). hsa-miR-135a-1 inhibits prostate cancer cell growth and migration by targeting EGFR. Tumour Biol. *37*, 14141–14151.
28. Ren, J.W., Li, Z.J., and Tu, C. (2015). MiR-135 post-transcriptionally regulates FOXO1 expression and promotes cell proliferation in human malignant melanoma cells. Int. J. Clin. Exp. Pathol. *8*, 6356–6366.
29. Wang, N., and Zhang, T. (2018). Downregulation of MicroRNA-135 Promotes Sensitivity of Non-Small Cell Lung Cancer to Gefitinib by Targeting TRIM16. Oncol. Res. *26*, 1005–1014.
30. Zhang, Y., Ren, S., Yuan, F., Zhang, K., Fan, Y., Zheng, S., Gao, Z., Zhao, J., Mu, T., Zhao, S., et al. (2018). miR-135 promotes proliferation and stemness of oesophageal squamous cell carcinoma by targeting RERG. Artif. Cells Nanomed. Biotechnol. *46*, 1210–1219.
31. Fan, P., Liu, L., Yin, Y., Zhao, Z., Zhang, Y., Amponsah, P.S., Xiao, X., Bauer, N., Abukiwan, A., Nwaeburu, C.C., et al. (2016). MicroRNA-101-3p reverses gemcitabine resistance by inhibition of ribonucleotide reductase M1 in pancreatic cancer. Cancer Lett. *373*, 130–137.
32. Liu, L., Salnikov, A.V., Bauer, N., Aleksandrowicz, E., Labsch, S., Nwaeburu, C., Mattern, J., Gladkich, J., Schemmer, P., Werner, J., and Herr, I. (2014). Triptolide reverses hypoxia-induced epithelial–mesenchymal transition and stem-like features in pancreatic cancer by NF-κB downregulation. Int. J. Cancer *134*, 2489–2503.
33. Zhao, Z., Bauer, N., Aleksandrowicz, E., Yin, L., Gladkich, J., Gross, W., Kaiser, J., Hackert, T., Strobel, O., and Herr, I. (2018). Intraductal papillary mucinous neoplasm of the pancreas rapidly xenografts in chicken eggs and predicts aggressiveness. Int. J. Cancer *142*, 1440–1452.